Focusing in multiwell potentials: Applications to ion channels

L. Ponzoni,[1] G. L. Celardo,[2] F. Borgonovi,[2] L. Kaplan,[3] and A. Kargol[4]
[1]*Dipartimento di Matematica e Fisica, Università Cattolica, via Musei 41, 25121 Brescia, Italy*
[2]*Dipartimento di Matematica e Fisica and Interdisciplinary Laboratories for Advanced Materials Physics, Università Cattolica, via Musei 41, 25121 Brescia, Italy and INFN, Sezione di Pavia, 27100 Pavia, Italy*
[3]*Department of Physics, Tulane University, New Orleans, Louisiana 70118, USA*
[4]*Department of Physics, Loyola University, New Orleans, Louisiana 70118, USA*
(Received 28 February 2013; published 28 May 2013)

We investigate nonequilibrium stationary distributions induced by stochastic dichotomous noise in double-well and multiwell models of ion channel gating kinetics. The channel kinetics is analyzed using both overdamped Langevin equations and master equations. With the Langevin equation approach we show a nontrivial focusing effect due to the external stochastic noise, namely, the concentration of the probability distribution in one of the two wells of a double-well system or in one or more of the wells of the multiwell model. In the multiwell system, focusing in the outer wells is shown to be achievable under physiological conditions, while focusing in the central wells has proved possible so far only at very low temperatures. We also discuss the strength of the focusing effect and obtain the conditions necessary for maximal focusing to appear. These conditions cannot be predicted by a simple master equation approach.

DOI: 10.1103/PhysRevE.87.052137 PACS number(s): 05.40.−a, 02.50.Ey, 82.20.Nk, 87.15.A−

I. INTRODUCTION

Interaction of physical, chemical, or biological systems with fluctuating stimuli, either random or periodic, has in recent years received much attention in a variety of contexts. It gives rise to new effects in nonlinear systems that cannot be observed under stationary perturbation. One of the most studied examples of such phenomena is stochastic resonance (SR) [1–13], an effect where noise with suitable properties, either intrinsic or added to the system, improves the system response to weak time-dependent signals. The signal-to-noise ratio can paradoxically be boosted by increasing the level of noise present in the system. Stochastic resonance was first suggested as an explanation for the cyclic ice ages observed in the earth's climate [1], but has been since expanded as a plausible explanation of various effects in other areas. Of particular interest is the application of SR to explain the detection of very weak signals in noisy environments observed in biological systems, e.g., in ion channels [3,5,6].

Another example is the dynamics of ratchets [14–16]. The term refers to spatially asymmetric potentials that, interacting with Brownian fluctuations, generate a directed drift in the system. The scale of the effect can be controlled by adjusting the properties of the noise. A similar ratchetlike effect has been observed in spatially symmetric potentials subject to temporally asymmetric noise (so-called correlation ratchets) [17].

An interesting example of such fluctuation-induced phenomena is called resonant activation [18–23]. It is an effect where diffusion over a fluctuating potential barrier is correlated with the fluctuation rate and a resonant effect is observed. As noted in Ref. [18], when the barrier fluctuations are slow compared to the natural time scale of barrier crossing, the behavior of the system can be described using an adiabatic approximation. In the opposite limit of very fast oscillations, the barrier crossing rate approaches that corresponding to the time-averaged barrier height. For intermediate barrier fluctuation rates, a resonancelike enhancement of the barrier crossing rate is observed. This has been applied, e.g., to chemical reaction rates [24] and to ion transport through channels [16,25].

A related effect, and the one we investigate in this paper, is the nonequilibrium kinetic focusing first proposed in Ref. [26]. It is an effect where a particle moving in a ratchetlike potential subject to external dichotomous noise fluctuations gets trapped in one of the energy wells. This mechanism was applied to gating kinetics of voltage-gated ion channels *in silico*, achieving a focusing of the channels into a particular conformational state corresponding to this energy well. The first experimental study of this effect in Shaker K^+ channels was reported in Ref. [27]. The phenomenon of particle trapping in a correlation ratchet has also been investigated [17].

Ion channels are membrane proteins in biological cells that form gated pores for a controlled exchange of physiologically important ions, such as sodium or potassium, between the cytosol and the extracellular medium [28]. Gating of voltage-gated ion channels is controlled by the transmembrane potential. These channels play a very important role in various physiological processes (nerve impulses, muscle contraction, etc.) and several human and animal disorders have been linked to malfunctioning ion channels. Therefore, there have been numerous studies aimed at advancing our understanding of channel gating kinetics and ultimately at controlling it. Kinetic focusing of ion channels seems to be very promising for both of these goals.

Gating kinetics of voltage-gated ion channels is a reflection of conformational changes of the channel molecule. From a physicochemical standpoint, the gating process has been modeled as a particle (so-called gating particle) moving in a certain multiwell energy landscape (describing the energy of molecular conformational states). Mathematically, the most commonly used description is a discrete Markov chain, where different Markov states correspond to minima in the energy profile and the transition rates between the states reflect the heights and widths of the energy barriers. The time evolution of the system is described by a master equation. These types

of models dominate the literature about ion channels and have been reasonably successful in explaining physiologically relevant effects (see, e.g., [29]). However, they are coarse approximations only, completely disregard intrawell motions of the gating particle, and work only if the energy barriers separating the wells are sufficiently high. More accurately, the process can be described by the overdamped Langevin equation [1].

In this paper we study both approaches to simple models of ion channel gating. In Sec. II we introduce the model. In Sec. III we analyze focusing in a two-state (two-well) model, which may represent an ion channel with two stable conformational states only: one open (where the ions can go through the cell membrane) and one closed. In the master equation approximation we find analytic expressions for the equilibrium probability in each well; however, we show that the master equation approach does not allow the conditions for maximal focusing to be obtained. These conditions may be obtained by including the leading Langevin correction to the master equation approximation. In Sec. IV we comment on a more realistic model of gating kinetics for a Shaker potassium channel developed by Bezanilla *et al.* [29] based on patch-clamping experiments with ionic and gating currents.

II. MODEL

In order to model the ion channel gating kinetics, we consider a one-dimensional potential energy landscape, where the potential minima are the possible states of the ion channel, while the barrier heights between two neighboring states are chosen so as to reproduce the correct transition rates. Within this model the dynamics of the ion channel can be described by the overdamped Langevin equation [26]

$$\gamma \dot{x}(t) = -u'(x) + \sqrt{2\gamma k_B T}\,\xi(t), \tag{1}$$

where $\xi(t)$ is a white noise with $\langle \xi(t) \rangle = 0$ and $\langle \xi(t)\xi(t') \rangle = \delta(t - t')$, $u(x)$ is the potential energy landscape, γ is the friction coefficient, T is the temperature of the bath, and k_B is the Boltzmann constant.

We investigate the effect of a time-dependent stochastic external potential on the out-of-equilibrium stationary distributions of our model. When an external voltage $v_{\rm ext}(t)$ is applied across the cell membrane, the particle behaves as if it had a charge valence z and the Langevin equation becomes (see [26])

$$\gamma \dot{x}(t) = -u'(x) + z v_{\rm ext}(t)/\lambda + \sqrt{2\gamma k_B T}\,\xi(t), \tag{2}$$

where the length scale λ is the cell membrane thickness. Using the rescaled variables

$$\begin{aligned} X &= \frac{zx}{\lambda}, \quad \tau = \frac{z^2 k_B T}{\gamma \lambda^2} t, \\ V_{\rm ext}(\tau) &= \frac{v_{\rm ext}(t)}{k_B T}, \quad U(X) = \frac{u(x)}{k_B T}, \end{aligned} \tag{3}$$

we finally get the Langevin equation in dimensionless form

$$\dot{X}(\tau) = -U'(X) + V_{\rm ext}(\tau) + \sqrt{2}\,\xi(\tau). \tag{4}$$

In the following we set $\gamma = \lambda = z = 1$ for convenience, so that $X = x$ and $\tau = k_B T t$. We see that the external membrane potential $V_{\rm ext}$ changes the potential shape in a linear way:

$$U(X) \to U(X) - V_{\rm ext} X. \tag{5}$$

The external potential will include a time-independent contribution plus a stochastic part given by dichotomous noise (DN):

$$V_{\rm ext}(\tau) = V_0 + V_{\rm DN}(\tau), \tag{6}$$

where V_0 is a constant and $V_{\rm DN}(\tau)$ represents a time-dependent random and asymmetric switching between two fixed values of the potential $V_\pm$,

$$V_+ = \sqrt{\frac{D}{\tau_v}\left(\frac{1+\epsilon}{1-\epsilon}\right)}, \quad V_- = -\sqrt{\frac{D}{\tau_v}\left(\frac{1-\epsilon}{1+\epsilon}\right)}, \tag{7}$$

with transition probabilities w_+ (from the $+$ to the $-$ state) and w_- (from the $-$ to the $+$ state),

$$w_+ = (1+\epsilon)/2\tau_v, \quad w_- = (1-\epsilon)/2\tau_v. \tag{8}$$

It is easy to show that such DN has a null time average

$$\langle V_{\rm DN}(\tau) \rangle = 0 \tag{9}$$

and correlation function

$$\langle V_{\rm DN}(\tau)\, V_{\rm DN}(0) \rangle = (D/\tau_v) \exp(-\tau/\tau_v),$$

so it can be fully characterized by three dimensionless parameters: correlation time τ_v, intensity D/τ_v (or amplitude $\sqrt{D/\tau_v}$), and asymmetry ϵ (with $-1 < \epsilon < 1$).

III. FOCUSING IN A DOUBLE-WELL POTENTIAL

The two-state model, introduced in this section, is intended to represent open and closed configurations. Even if it is too simple to adequately represent the behavior of real channels, it is commonly used as a toy model to demonstrate various phenomena [12,13,22,24,30–33]. A two-state model can also be understood as a submodel of a larger system (see Sec. IV).

The double-well potential landscape considered here is

$$u(x) = -\tfrac{1}{2} a x^2 + \tfrac{1}{4} b x^4; \tag{10}$$

it has two minima at $\pm x_m = \pm\sqrt{a/b}$ and a central barrier with height $\Delta u = a^2/4b$ at $x_b = 0$ (see the solid curve in Fig. 1). Due to thermal fluctuations, the particle jumps between the two wells with a rate that, for $\Delta u/k_B T \gg 1$, is given by the Kramers formula [1]

$$w_K = \frac{\omega_0 \omega_b}{2\pi\gamma} \exp\left(-\frac{\Delta u}{k_B T}\right), \tag{11}$$

where $\omega_0^2 = |u''(x_m)|$ and $\omega_b^2 = |u''(x_b)|$. If we now add a DN perturbation with $V_0 = 0$ [see Eq. (6)], then depending on the state of the DN, there are two possible configurations for the potential: a $(-)$ configuration and a $(+)$ configuration, as depicted in Fig. 1.

A. Solving the Langevin equation

To study the stationary probability distribution, one has to solve the stochastic equation (4) numerically. We do so using an order 1.5 strong Ito-Taylor scheme (in explicit form), as described by Kloeden and Platen [34]. Starting with randomly chosen initial positions and integrating the Langevin equation

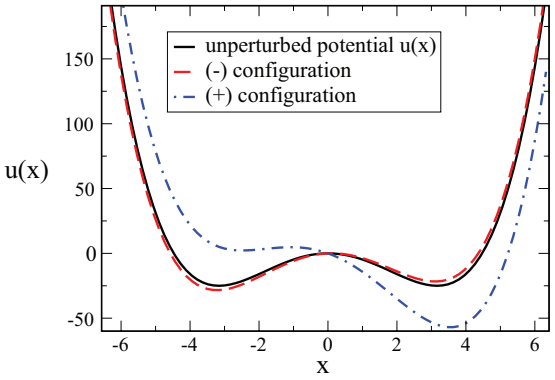

FIG. 1. (Color online) Unperturbed double-well potential $u(x)$ of Eq. (10) and the two configurations of the potential when it is modified by dichotomous noise with $V_0 = 0$, as indicated in the legend. The potential parameters are $a = 10$ and $b = 1$, while the DN shown is given by $D/\tau_v = 0.71$, $k_BT = 0.15\Delta u$, and $\epsilon = 0.8$.

forward in time, we compute the probabilities $P_{L/R}(\tau)$ of finding the gating particle in each potential well at time τ. We have verified that after a transient time, these probabilities always reach stationary values $P^{\rm eq}_{L/R}$ dependent on the DN parameters.

The results of integrating the Langevin equation are shown as data points (circles) in Fig. 2, where we fix the DN intensity D/τ_v and asymmetry ϵ and vary the DN correlation time τ_v. Each data point in the graph represents the left well equilibrium probability $P^{\rm eq}_L$. As one can see, $P^{\rm eq}_L$ reaches a minimum of approximately 10% at a specific value of τ_v (i.e., 90% of probability is concentrated in the right well). This is nonequilibrium kinetic focusing and it should not be confused with the trivial focusing that occurs at large τ_v ($P^{\rm eq}_L = P^{\rm mean}_L \approx 0.8$), which can be understood based on equilibrium considerations.

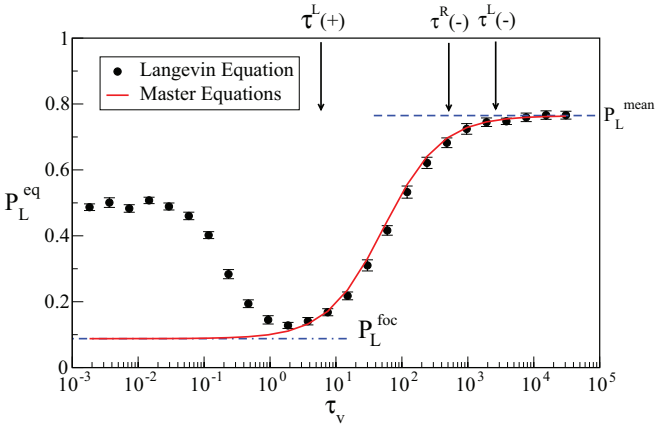

FIG. 2. (Color online) Equilibrium probability in the left well versus the DN correlation time τ_v. The data points (circles) are obtained from the Langevin equation, while the solid curve is obtained from a master equation approach (see Sec. III B). Thermal tunneling times $\tau^{L,R}(\pm)$ are shown as arrows [except for $\tau^R(+) \sim 10^6$, which is off the scale of the graph]. The horizontal dashed line represents the limit $P^{\rm mean}_L$, computed with Eq. (14), while the dot-dashed horizontal line is $P^{\rm foc}_L$ [see Eq. (25)]. Here we have $D/\tau_v = 0.71$, $k_BT = 0.15\Delta u$, and $\epsilon = 0.8$ as in Fig. 1.

We would now like to understand the relevant time scales in this system. Since the DN causes the potential to switch between two configurations, it is possible to define four thermal tunneling times in the system: $\tau^{L/R}(+/-)$, where, for example, $\tau^L(+)$ is the mean time after which a particle jumps from the left to the right well when the potential is in the $(+)$ configuration (that is, when $V_{\rm DN} = V_+$). Note that in this section we consider a physically realistic regime in which both the DN amplitude and the thermal fluctuations are not too large compared to the height of the potential barrier. Moderate thermal fluctuations relative to the potential barrier correspond to physiological conditions at room temperature for ion channels [26]. Moreover, a moderate DN amplitude corresponds to an experimentally realistic regime since a large amplitude would interfere with the electrophysiological properties of cell membranes and of the ion channels in the membranes. Under these assumptions, the thermal tunneling times are given by the inverses of the tunneling rates $w^{R/L}(\pm)$, obtained by applying Eq. (11) to the perturbed potential, so that we have

$$\tau^{L/R}(\pm) = \frac{1}{w^{L/R}(\pm)}. \tag{12}$$

We should also take into account two additional characteristic times, given by the DN, namely,

$$\tau^{\pm}_v = \frac{1}{w_\pm} = \frac{2}{(1\pm\epsilon)}\tau_v, \tag{13}$$

where $w_\pm$ are given by Eq. (8). The scales $\tau^{\pm}_v$ are estimates of the typical times spent in each configuration between DN switchings.

When the DN switching times $\tau^{\pm}_v$ are much larger than the thermal tunneling times $\tau^{L,R}(\pm)$, we can assume that the system reaches thermal equilibrium separately in each potential configuration. Therefore, if $P^{\rm eq}_{L/R}(\pm)$ are the thermal Gibbs probabilities for each well in the $(+)$ and $(-)$ configurations, then it is reasonable to assume that, for $\tau^{\pm}_v \to \infty$, the probability $P^{\rm eq}_L$ approaches the mean value

$$P^{\rm eq}_L \to \frac{\tau^+_v}{(\tau^+_v + \tau^-_v)} P^{\rm eq}_L(+) + \frac{\tau^-_v}{(\tau^+_v + \tau^-_v)} P^{\rm eq}_L(-) \equiv P^{\rm mean}_L. \tag{14}$$

The $P^{\rm mean}_L$ is shown as the dashed horizontal line in Fig. 2 and agrees very well with numerical data.

In the opposite limit of fast DN switching ($\tau_v \to 0$), the probability distribution becomes symmetric:

$$P^{\rm eq}_L, P^{\rm eq}_R \to 1/2, \tag{15}$$

which is the value obtained with our numerical simulations of the Langevin equation (see Fig. 2). The limit $\tau_v \to 0$ of the Langevin equation can be understood by noting that when the switching between potential configurations is fast compared to the time scale on which the particle moves in the potential, the particle effectively sees only the time-averaged DN potential, which is zero in our case [see Eq. (9)]. This can be seen explicitly by assuming for simplicity a periodic, rather than stochastic, switching between the two potential configurations. Indeed, the displacement of the particle after time τ^+_v in the

(+) configuration is [see Eq. (4)]

$$(\Delta X)^+ = [-U'(X) + V_+ + \sqrt{2}\,\xi]\tau_v^+ \tag{16}$$

and after time τ_v^- in the (−) configuration we have the additional displacement

$$(\Delta X)^- = [-U'(X) + V_- + \sqrt{2}\,\xi]\tau_v^-, \tag{17}$$

neglecting the terms proportional to $\tau_v^+\tau_v^-$. The total displacement after a time $\tau_v^+ + \tau_v^-$ is then

$$\begin{aligned}\Delta X &= (\Delta X)^+ + (\Delta X)^- \\ &= [-U'(X) + \sqrt{2}\,\xi](\tau_v^+ + \tau_v^-) + (V_+\tau_v^+ + V_-\tau_v^-)\end{aligned} \tag{18}$$

and, dividing by $\tau_v^+ + \tau_v^-$, we get the Langevin equation for an infinitely fast oscillating potential:

$$\dot{X} = -U'(X) + \sqrt{2}\,\xi + \frac{V_+\tau_v^+ + V_-\tau_v^-}{\tau_v^+ + \tau_v^-}. \tag{19}$$

The last term corresponds to the time average of the DN.

In the regime of intermediate values of τ_v, we observe a nontrivial focusing effect (see Fig. 2). This is an interesting result since the applied DN has zero mean [Eq. (9)] and nevertheless can induce a stationary distribution that focuses the system in one well.

B. Master equation approach

In order to understand the conditions for the focusing, we attempt a simple explanation through a master equation approach

$$\dot{\mathbf{P}} = W\mathbf{P}. \tag{20}$$

Here

$$\mathbf{P}(\tau) = \begin{pmatrix} P_L(+) \\ P_L(-) \\ P_R(+) \\ P_R(-) \end{pmatrix}$$

is the vector of probabilities [e.g., $P_L(+)$ is the joint probability of the DN potential being in the (+) configuration and the particle being in the left well at time τ] and W is the 4×4 transition matrix

$$W = \begin{pmatrix} -w_+ - w^L(+) & w_- & w^R(+) & 0 \\ w_+ & -w_- - w^L(-) & 0 & w^R(-) \\ w^L(+) & 0 & -w_+ - w^R(+) & w_- \\ 0 & w^L(-) & w_+ & -w_- - w^R(-) \end{pmatrix}, \tag{21}$$

where, for example, in the upper left matrix element $W_{L(+),L(+)} = -w_+ - w^L(+)$ the first term represents the probability of switching from $L(+)$ to $L(-)$, with the rate given in Eq. (8), and the second term represents the probability of tunneling from $L(+)$ to $R(+)$, with the appropriate tunneling rate in the (+) configuration. Setting the left-hand side of Eq. (20) to zero and imposing the normalization condition $P_L(+) + P_L(-) + P_R(+) + P_R(-) = 1$, we obtain analytically the equilibrium probabilities in terms of the switching time τ_v, the asymmetry ϵ, and the four tunneling rates. In particular,

$$P_L^{\rm eq} = P_L^{\rm eq}(+) + P_L^{\rm eq}(-) = \frac{\tilde{w}^R}{\tilde{w}^R + \tilde{w}^L}, \tag{22}$$

where

$$\begin{aligned}\tilde{w}^R = {} & w^R(-)(1+\epsilon)[1 + \tau_v w^L(+)] \\ & + w^R(+)(1-\epsilon)[1 + \tau_v w^L(-)] \\ & + 2\tau_v w^R(+)w^R(-)\end{aligned} \tag{23}$$

and

$$\begin{aligned}\tilde{w}^L = {} & w^L(-)(1+\epsilon)[1 + \tau_v w^R(+)] \\ & + w^L(+)(1-\epsilon)[1 + \tau_v w^R(-)] \\ & + 2\tau_v w^L(+)w^L(-)\end{aligned} \tag{24}$$

may be interpreted as being proportional to the effective transition rates from right to left and from left to right, respectively. Of course, $P_R^{\rm eq}$ is given by $P_R^{\rm eq} = 1 - P_L^{\rm eq}$.

In Fig. 2 we compare the results obtained using the Langevin equation with those obtained via the master equation (22). We observe good agreement between the two approaches when the DN correlation time τ_v is larger than the value at which the best focusing occurs: indeed, for large τ_v, Eq. (22) manifestly reduces to the result $P_L^{\rm eq} = P_L^{\rm mean}$ obtained using the Langevin equation in the same limit [Eq. (14)]. In contrast, for $\tau_v \to 0$, the master equation gives a completely different result. In fact, we see from Fig. 2 that the master equation implies that maximal focusing is attained for infinitely fast switching ($\tau_v \to 0$), whereas in reality focusing is entirely absent in this limit. Explicitly, in the fast-switching limit $\tau_v \to 0$, Eq. (22) reduces to

$$P_L^{\rm eq} = P_L^{\rm foc} \equiv \frac{\langle w^R\rangle}{\langle w^L\rangle + \langle w^R\rangle}, \tag{25}$$

where

$$\langle w^{L/R}\rangle = \frac{1+\epsilon}{2}w^{L/R}(-) + \frac{1-\epsilon}{2}w^{L/R}(+). \tag{26}$$

Equation (25) may also be obtained directly by noting that for small τ_v the master equation implies equilibration between the $L(+)$ and $L(-)$ states and separately between the $R(+)$ and $R(-)$ states, with slow transitions between L and R being

governed by the DN-averaged rates $\langle w^{L/R}\rangle$. In other words, the $\tau_v \to 0$ limit of the master equation corresponds not to motion in a DN potential averaged over the (+) and (−) configurations, but to dynamics using tunneling rates averaged over two configurations. The time-averaged transition rates are not equal in general and thus do not lead to equal probabilities in the two wells, even though the time-averaged potential vanishes. This is a limitation of the master equation formalism. An intuitive explanation of the failure of the master equation approach for $\tau_v \to 0$ is that the system does not have time to equilibrate in each well before the switching and thus the two-state model for the two wells becomes inappropriate.

In Fig. 2 the value of $P_L^{\rm foc}$ is shown to agree with the master equation solution in the limit $\tau_v \to 0$ and, interestingly, it is close to the focusing value of $P_L^{\rm eq}$ at the minimum. This behavior will be explained below and used to determine the dependence of the focusing intensity on the parameters of the model. The fact that a master equation approach cannot explain the focusing shows that the focusing is highly nontrivial, being a truly nonequilibrium effect.

C. Understanding the focusing conditions

To better understand the conditions for nonequilibrium focusing we need to consider the interplay of several time scales. Without loss of generality we can assume, as in Eqs. (5) and (7), that in the (+) configuration the DN potential has a downward slope, so that the tunneling rate from left to right is greater than the tunneling rate from right to left in this configuration. Consequently, due to the zero average of the DN potential, the opposite must be true in the (−) configuration. Since we are interested in nonequilibrium focusing, the switching time τ_v will be short compared to the tunneling times $\tau^{L/R}(\pm)$. At the same time, we want the switching time τ_v to be sufficiently large that the master equation gives at least a reasonable first-order approximation to the true equilibrium probabilities obtained from the Langevin equation. This requires that τ_v is large compared to the typical time scale $\tau_{\rm well}$ associated with Langevin equilibration in a single well; $\tau_{\rm well}$ can be evaluated from the Langevin equation (4), as the time it takes for oscillations to be damped, so that we have $\tau_{\rm well} = 1/U''(X_m) = k_BT/u''(x_m)$, where X_m is the value at which the potential is minimized [for the two-well model of Eq. (10) without DN perturbation $\tau_{\rm well} = \frac{a}{8b}\frac{k_BT}{\Delta u}$]. Thus we have

$$\begin{aligned} &\tau_{\rm well} \ll \tau_v \ll \tau^L(+) \ll \tau^R(+), \\ &\tau_{\rm well} \ll \tau_v \ll \tau^R(-) \ll \tau^L(-). \end{aligned} \tag{27}$$

In this nonequilibrium regime, the rates $w^L(+)$ and $w^R(-)$ dominate the transitions between the two wells. In particular, in the regime given by (27), the equilibrium probability to be in the left well is given to leading order by omitting the very small rates $w^R(+)$ and $w^L(-)$ from Eq. (25), i.e.,

$$\begin{aligned} P_L^{\rm eq} = P_L^{\rm foc} &= \frac{(1+\epsilon)w^R(-)}{(1+\epsilon)w^R(-)+(1-\epsilon)w^L(+)} \\ &= \frac{(1+\epsilon)\tau^L(+)}{(1+\epsilon)\tau^L(+)+(1-\epsilon)\tau^R(-)}. \end{aligned} \tag{28}$$

Now including the first-order corrections to the small-τ_v behavior of the master equation and also the first-order correction to the validity of the master equation result (i.e., the leading-order correction to the master equation equilibrium probabilities as given by the Langevin equation for nonzero $\tau_{\rm well}/\tau_v$), we have

$$\begin{aligned} P_L^{\rm eq} = &\frac{(1+\epsilon)\tau^L(+)}{(1+\epsilon)\tau^L(+)+(1-\epsilon)\tau^R(-)} \\ &+ O\left(\frac{\tau_v}{\tau^L(+)}\right) + O\left(\frac{\tau_v}{\tau^R(-)}\right) + O\left(\frac{\tau_{\rm well}}{\tau_v}\right). \end{aligned} \tag{29}$$

Focusing in the right well will be possible when $(1+\epsilon)\tau^L(+) \ll (1-\epsilon)\tau^R(-)$ and similarly focusing in the left well will be possible when $(1+\epsilon)\tau^L(+) \gg (1-\epsilon)\tau^R(-)$. Without loss of generality, we will concentrate on the case where the system parameters permit focusing in the right well, as in Fig. 2, so

$$(1+\epsilon)\tau^L(+) \ll (1-\epsilon)\tau^R(-). \tag{30}$$

We are now ready to determine the switching rate necessary for maximal focusing. Rewriting Eq. (29) and dropping the $1/\tau^R(-)$ correction term, we have

$$P_L^{\rm eq} = P_L^{\rm foc}\left[1 + C_1\frac{\tau_v}{\tau^L(+)} + C_2\frac{\tau_{\rm well}}{\tau_v}\right], \tag{31}$$

where C_1 and C_2 are dimensionless constants independent of τ_v, $\tau^L(+)$, and $\tau_{\rm well}$. In particular, we easily find $C_1 = 1$ by expanding Eq. (22) to first order in τ_v.

Minimizing $P_L^{\rm eq}$ as a function of τ_v, we find the optimal switching time

$$\tau_{v\,\rm min} = \sqrt{C_2\tau_{\rm well}\tau^L(+)} \tag{32}$$

and the optimal focusing

$$P_{L\,\rm min}^{\rm eq} = P_L^{\rm foc}\left[1 + 2\sqrt{C_2\frac{\tau_{\rm well}}{\tau^L(+)}}\right]. \tag{33}$$

Interestingly, even though the master equation fails entirely in the $\tau_v \to 0$ limit and is wholly inadequate for determining the condition (32) for optimal nonequilibrium focusing, the strength of optimal focusing is well approximated by the simple analytic expression $P_L^{\rm foc}$ [Eq. (25)], obtained using the master equation in this limit.

In Fig. 3 we study numerically how the switching time $\tau_{v\,\rm min}^+ = \frac{2}{1+\epsilon}\tau_{v\,\rm min}$, at which a minimum of $P_L^{\rm eq}$ is found, depends on the thermal tunneling time $\tau^L(+)$ for different values of the asymmetry ϵ, the intensity D/τ_v, and the temperature T. In each data set, D/τ_v and k_BT are fixed and the asymmetry parameter ϵ is varied. Every value of $\tau_{v\,\rm min}^+$ is then computed from a graph like Fig. 2, by fitting the function $P_L^{\rm eq}[\ln(\tau_v)]$ to a quadratic form around its minimum. A universal curve is obtained, with precisely the scaling $\tau_{v\,\rm min}^+ \propto \sqrt{\tau^L(+)}$ predicted by Eq. (32). Furthermore, we have the remarkable result that $\tau_{v\,\rm min}^+$ to a very good approximation depends on the noise amplitude, asymmetry, and temperature only through $\tau^L(+)$. This is initially surprising, since the single-well equilibration time $\tau_{\rm well}$ and the C_2 coefficient in Eq. (32) are also expected to vary with these parameters and additionally the factor $2/(1+\epsilon)$ relating $\tau_{v\,\rm min}^+$ and $\tau_{v\,\rm min}$ depends explicitly on ϵ. We note, however, that the tunneling

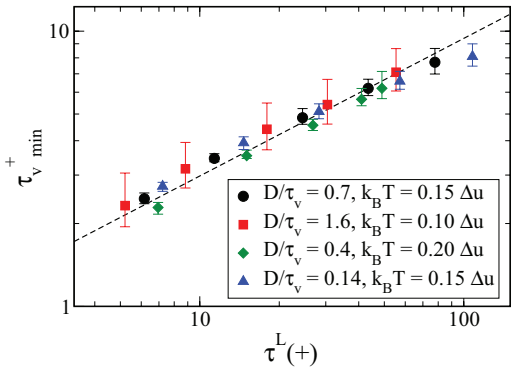

FIG. 3. (Color online) Correlation time $\tau_{v\,\mathrm{min}}^{+}$, for which we observe the strongest focusing, plotted as a function of the transition time $\tau^{L}(+)$. Each data set consists of simulations with fixed DN intensity D/τ_v and temperature T, as indicated in the legend, and varying ϵ. The dashed line indicates a square root dependence. Error bars describe the variation of $\tau_{v\,\mathrm{min}}^{+}$ for which P_L^{eq} changes by 0.1% from its minimum value.

time $\tau^{L}(+)$ is the only quantity in Eq. (32) that exhibits exponential sensitivity to the system parameters and so it is reasonable that the variation of $\tau^{L}(+)$ should be the leading effect.

Up to now, we have only studied the probability distribution induced by the DN as a function of τ_v. Now we analyze the dependence of the focusing on the other parameters, specifically ϵ and k_BT. In Fig. 4 (top panel) we show the left well probability P_L^{eq} at strongest focusing vs the DN asymmetry parameter ϵ. We observe that the focusing gets weaker as the asymmetry decreases ($\epsilon \to 0$). This can be explained by noting that the separation of scales between the

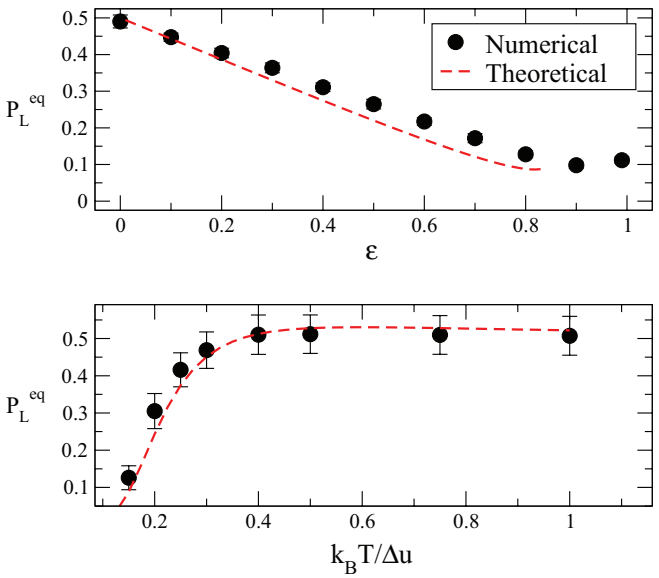

FIG. 4. (Color online) The top panel shows P_L^{eq} at the strongest focusing (circles) plotted vs ϵ for fixed $D/\tau_v = 0.71$ and $k_BT = 0.15\Delta u$. The bottom panel shows P_L^{eq} at the strongest focusing (circles) plotted vs $k_BT/\Delta u$ for $D/\tau_v = 0.016(\Delta u/k_BT)^2$ and fixed $\epsilon = 0.8$. In both panels the dashed curve represents the theoretical prediction [Eq. (25)] obtained from the master equation (see the text).

two thermal tunneling times $\tau^{L}(+)$ and $\tau^{R}(-)$ decreases as the asymmetry decreases and therefore the condition (30) for focusing in the right well is not met.

In Fig. 4 (bottom panel) we show the left well probability P_L^{eq} at strongest focusing vs the temperature. Obviously increasing the temperature destroys the focusing effect. This is expected since increasing temperature causes the single-well equilibration time τ_{well} to grow while all the tunneling times $\tau^{L,R}(\pm)$ are shortened and additionally the separation of scales between the different tunneling times is reduced. All of these effects combine to make the conditions in Eq. (27) more difficult to satisfy at higher temperature.

We recall from Eq. (33) that although the master equation fails to fit the data for very fast switching, specifically when τ_v becomes comparable with the single-well equilibration time τ_{well}, the equilibrium probability P_L^{foc} obtained from the master equation in this limit is a good leading-order estimate for the strength of maximal focusing. This remains true as long as τ_{well} is small compared to the smallest tunneling time, i.e., as long as there is a separation of time scales between equilibration in a single well and interwell tunneling. Thus we can use Eq. (25) to analytically estimate the value of the focusing as a function of the parameters. This analytical result is shown in both panels of Fig. 4 as a dashed curve and is in good agreement with our numerical results, except when the asymmetry ϵ or k_BT becomes so large that the energy barriers are not well defined [and the Kramers formula (11) is no longer applicable].

The results of our investigations on a double-well potential can be summarized as follows.

(i) A stochastic perturbing potential with zero time average can induce an unbalanced stationary probability distribution between the two wells.

(ii) Conditions for right-well focusing are $\tau_{\mathrm{well}} \ll \tau_v \ll \tau^{L}(+) \ll \tau^{R}(-) \ll \tau^{L}(-) \ll \tau^{R}(+)$ [see Eqs. (27) and (30)] and similarly for left-well focusing.

(iii) The master equation approach completely fails for fast DN perturbations (small τ_v) and is unable to describe the conditions for nonequilibrium kinetic focusing.

(iv) The conditions for maximal focusing can be obtained by adding the leading Langevin correction to the master equation equilibrium probabilities. The optimal switching time τ_v scales as $\sqrt{\tau_{\mathrm{well}}\tau^{L}(+)}$ for right-well focusing [see Eq. (32)].

(v) At fixed DN intensity, the focusing can be improved by increasing the asymmetry ϵ or decreasing the temperature. Analytical estimation of the focusing intensity is given by Eq. (25).

IV. EIGHT-WELL POTENTIAL: A MORE REALISTIC MODEL FOR ION CHANNEL GATING

In the previous section we showed that it is possible to modify the stationary probability distribution in a double-well potential, and particularly to increase the probability to find the system in one well, by introducing a stochastic perturbation. Although two-well potentials can be useful toy models, they are typically far too simple to describe the gating of real ion channels. As an example we consider a very well-studied voltage-gated ion channel, the Shaker K^+ channel. There have been numerous models developed for the Shaker channel gating kinetics based on available experimental

$$C_0 \underset{\alpha_0}{\overset{\beta_0}{\rightleftharpoons}} C_1 \underset{\alpha_1}{\overset{\beta_1}{\rightleftharpoons}} C_{11} \underset{\alpha_1}{\overset{\beta_1}{\rightleftharpoons}} C_{12} \underset{\alpha_1}{\overset{\beta_1}{\rightleftharpoons}} C_2 \underset{\alpha_2}{\overset{\beta_2}{\rightleftharpoons}} C_3 \underset{\alpha_3}{\overset{\beta_3}{\rightleftharpoons}} C_4 \underset{\alpha_4}{\overset{\beta_4}{\rightleftharpoons}} O$$

FIG. 5. The BPS model [29]. Forward and backward tunneling rates α_i and β_i, respectively, were determined by fitting to various types of experimental electrophysiological data (ionic and gating currents from patch-clamping experiments) and can be found in Ref. [29].

data from patch-clamping experiments. A vast majority of them have the form of a discrete Markov chain characterizing possible conformational states of the channel molecule and the transitions between the states. As in Ref. [26], we concentrate on the Bezanilla-Perozo-Stefani (BPS) model, proposed in Ref. [29]. It is a Markov chain of eight states as shown schematically in Fig. 5. The C states are closed and the O state represents an open conformation of the channel in which the ions can pass through the pore. We label the states 1–8, left to right.

Since transitions occur only between nearest-neighbor states, the ion channel can be represented by an eight-well potential landscape $u(x)$, as depicted in Fig. 6. The eight potential minima are the possible states of the channel and the barrier heights are chosen so to reproduce the correct experimental transition rates. The piecewise-linear shape of the energy landscape was chosen for computational simplicity, as the exact shape is not known.

In the following we present some preliminary discussion of the effect of stochastic noise on multistate models, described by such multiwell potential landscapes, leaving a deeper analysis for future work.

The problem of focusing in such an eight-well model has previously been considered by Millonas and Chialvo [26]. Based on a probabilistic treatment of the Langevin equation (4), they concluded that for very low temperature and large amplitude of the DN, it is possible to induce stationary probability distributions concentrated in an arbitrarily chosen potential well. This effect has been called the nonequilibrium kinetic focusing. The problem is that the two conditions (very low temperature and large DN) are not physiological, since no living organism can function at such extreme temperatures,

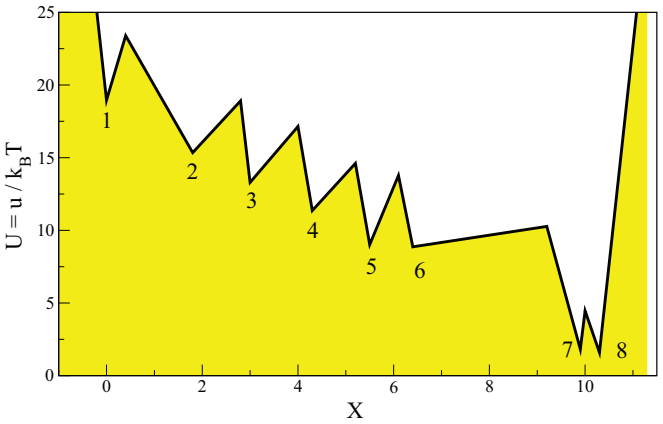

FIG. 6. (Color online) Potential u used by Millonas and Chialvo in Ref. [26] as a model of the Shaker K^+ channel. For the definition of the rescaled potential $U(X)$, see Eq. (3). Here we assume $T = 300$ K.

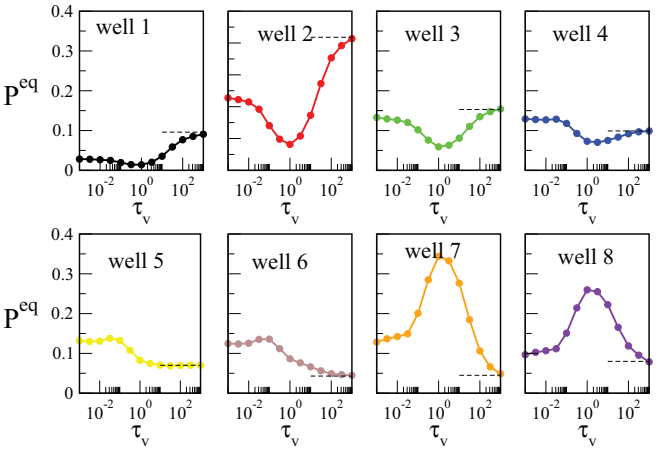

FIG. 7. (Color online) Equilibrium probabilities $P_i^{\rm eq}$ in the ith well shown as functions of the DN correlation time τ_v. The parameters are $D/\tau_v = 1$, $\epsilon = 0.8$, $V_0 = \langle V_{\rm ext}\rangle = (-45\ {\rm mV})/k_BT$, and $T = 300$ K. Dashed lines represent stationary probabilities given by Eq. (34).

and very large voltage fluctuations tend to destroy the cell membrane in which the ions are embedded. Hence Millonas and Chialvo's result could not be verified experimentally.

For this reason, we investigate numerically whether nonequilibrium kinetic focusing can occur in an eight-well potential under physiological conditions (room temperature and moderate DN amplitude), i.e., under the conditions studied in the previous section in a two-well case. We also compare the analytical predictions of Ref. [26] for low temperature and large DN intensity with our numerical simulations.

A. Room temperature and low DN intensity

Similar to the results of the previous section, we consider the overdamped Langevin equation (4) and compute the equilibrium probabilities $P_i^{\rm eq}$ for each of the eight wells, defined as in the previous sections. Figure 7 shows typical results of our simulations of the equilibrium probability distribution $P_i^{\rm eq}$ for each well i as a function of τ_v, at fixed asymmetry ϵ, intensity D/τ_v, and mean external potential V_0.

It is clear from the figure that as τ_v varies strong focusing only occurs in wells 7 and 8 for intermediate values of τ_v and also in well 2 for large τ_v. The equilibrium probabilities of the other wells are less strongly dependent on τ_v for the chosen values of the parameters. We can also draw conclusions similar to those obtained for the double-well case in the limits of very small and very large τ_v. For very fast DN switching ($\tau_v \to 0$), the system responds to the average potential and the probability distribution is given by the thermal Gibbs distribution for $V_{\rm ext} = V_0$, so the focusing effect should be judged by comparing the probability at finite τ_v with the probability for $\tau_v \to 0$. In contrast, for τ_v large compared to the tunneling times, the stationary probabilities (see dashed horizontal lines in Fig. 7) can be evaluated, as in Eq. (14), by

$$P_i^{\rm mean} = \frac{\tau_v^+}{(\tau_v^+ + \tau_v^-)} P_i(+) + \frac{\tau_v^-}{(\tau_v^+ + \tau_v^-)} P_i(-), \qquad (34)$$

where the probabilities $P_i(\pm)$ are the thermal Gibbs probabilities for each well in the $(+)$ and $(-)$ configurations.

The nontrivial focusing in the intermediate τ_v regime resembles that found in the double-well case. Indeed, the conditions discussed in Sec. III C seem to work also in the multiwell case, but they need to be generalized. We note that focusing in an inner well i requires the conditions to hold on both sides, i.e.,

$$\tau_{\text{well}} \ll \tau_v \ll \tau^{i-1,i}(+), \tau^{i+1,i}(-), \quad (35)$$

$$\tau^{i-1,i}(+) \ll \tau^{i,i-1}(-) \ll \tau^{i-1,i}(-) \ll \tau^{i,i-1}(+), \quad (36)$$

$$\tau^{i+1,i}(-) \ll \tau^{i,i+1}(+) \ll \tau^{i+1,i}(+) \ll \tau^{i,i+1}(-), \quad (37)$$

where $\tau^{i,j}(\pm)$ is the tunneling time from well i to neighboring well j in the $(\pm)$ configuration. The dual set of conditions is of course more difficult to satisfy in practice; this is especially true at room temperature when the separation between the time scales is less pronounced, as discussed in Sec. III C.

In the BPS model, we find that it is appropriate to treat the two wells 7 and 8 as a single unit since the four dimensionless tunneling times $\tau^{7,8}(\pm)$ and $\tau^{8,7}(\pm)$ are all found numerically to be less than 0.5 at room temperature, while the other tunneling times mostly range between 1 and 100. We then see that focusing in the 7-8 unit may be possible when $\tau^{6,7}(+) \ll \tau^{7,6}(-) \ll \tau^{6,7}(-) \ll \tau^{7,6}(+)$; this condition is indeed satisfied at room temperature. Nevertheless, a more detailed analysis is necessary to understand fully how to relate the focusing in the double well with that in the multiwell case.

These simulations were repeated with different values of the DN asymmetry parameter ϵ and of the DN intensity D/τ_v. In all cases we observed only some probability increase in the outer wells and despite multiple attempts we were not able to obtain focusing in the central wells. This negative result is very unfortunate since such focusing would be desirable as an effective tool for controlling the ion channel kinetics using stochastic perturbations.

B. Low temperature and large DN intensity

An analytical solution for the stationary probability distribution induced by a DN [Eq. (7) in Ref. [26]] was derived under the following assumptions.

(i) The amplitude of the driving must be larger than the maximal force associated with the potential, i.e., $\sqrt{D/\tau_v} > \sup|U'|$.

(ii) The potential barriers must be much larger than the thermal fluctuation energy $k_B T$.

The above two conditions imply, of course, that the driving is strong compared to thermal fluctuations. When we computed the probability distribution at room temperatures in Sec. IV A, we did not satisfy these two conditions required in Ref. [26], the main reason being that they were not physiologically feasible. Nevertheless, in this section we take this regime into consideration in order to understand the range of validity of the analytical prediction given in Ref. [26].

We have computed the probability distribution among the eight potentials wells for several different, but very low, temperatures while keeping the other parameters constant. In Fig. 8 we compare our numerical results (bars) with the results of the analytical formula from [26] (diamonds). The values of

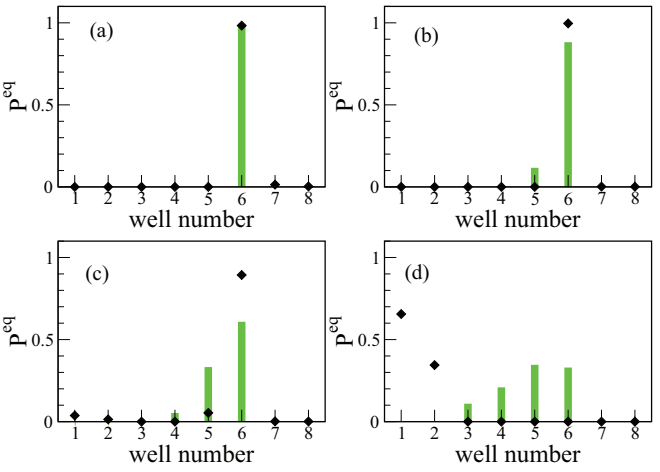

FIG. 8. (Color online) Probability distributions at different values of the temperature are computed with the Langevin equation (green bars) and theoretically (black diamonds) using Eq. (7) in Ref. [26]. The parameters are $D/\tau_v = 10^5$, $\epsilon = 0.6$, $\tau_v = 10^{-4}$, and $V_0 = -142\ \text{mV}/k_B T$. The temperature is (a) $T = 20$ K, (b) $T = 25$ K, (c) $T = 30$ K, and (d) $T = 40$ K.

the temperature and other relevant parameters are given in the figure caption.

As one can see, while there is good agreement at the lowest temperatures [Figs. 8(a) and 8(b)], the analytical formula for the probability distribution derived in Ref. [26] becomes less accurate as the temperature is increased [Figs. 8(c) and 8(d)] and fails completely at $T = 40$ K, well before room temperature is reached. Also, the numerical solutions to the Langevin equation show some degree of focusing at all temperatures considered, but the effect becomes progressively less pronounced as the temperature grows. This is in accord with our observations in Sec. IV A, where we failed to find any indication of focusing in the central wells at room temperature. Interestingly, in some cases we do notice significant focusing in the central wells even when the conditions of Millonas and Chialvo are not satisfied: For example, in Fig. 8(c), the Langevin equation yields a total probability of approximately 90% in wells 5 and 6, even though the conditions for the analytical equation of Ref. [26] fail. The presence of focusing in this case suggests that the conditions given in Ref. [26] are not necessary in order to achieve focusing.

V. CONCLUSION

The purpose of this work was to investigate the effect of nonequilibrium kinetic focusing, i.e., of selective enhancement of probability in one of the wells of a multiwell system, postulated by Millonas and Chialvo [26]. We tested for the presence of the effect in different parameter regimes (different temperatures and properties of the stochastic DN stimulation) and studied the necessary conditions for focusing.

We considered two different kinetic models of ion channels subjected to a dichotomous noise perturbation. The first was a simple model consisting of two wells separated by an energy barrier, while the second was a physiologically relevant eight-well model proposed by Bezanilla *et al.* [29] for the Shaker K^+ channel. The two models were studied numerically

using the master equation and the Langevin equation. For the double-well model, nonequilibrium focusing has been found under physiological conditions (room temperature and moderate external perturbation intensity) using the Langevin equation approach. Interestingly, the master equation failed for short DN correlation time and we observed a significant divergence between the results of the two methods. It clearly indicates that the master equation approach, dominant in biophysical literature on ion channel gating kinetics, has significant limitations. For the eight-well model, nonequilibrium focusing was observed under physiological conditions, but only in the outer wells (wells 1, 2, 7, and 8). Focusing in the central wells, described by Millonas and Chialvo [26], was observed only at low temperatures, in the nonphysiological regime. We also investigated the existence of this phenomenon and the dependence of focusing strength on the external perturbation parameters. In the double-well case we suggested the necessary conditions, while in the eight-well case more analysis is needed in order to address this question.

We also analyzed the results of Millonas and Chialvo in Ref. [26] obtained under the assumption that $T \to 0$. We showed that their analytical formula for the nonequilibrium kinetic focusing starts to fail well before physiological conditions (room temperature and moderate external perturbation intensity) are achieved. It also seems that the conditions for focusing given in Ref. [26] are overly restrictive, since we observed meaningful focusing outside that regime, albeit still far away from physiologically relevant conditions.

In perspective, our analysis still leaves open the question of whether it is possible to focus an ion channel in an arbitrarily chosen well, thus completely controlling its dynamics, under physiological conditions. This is a prospect that would be very interesting from a practical point of view. Although we failed to see focusing in any of the central wells under physiological conditions, we still do not know if this could be possible with a properly chosen stochastic stimulation. Nevertheless, we have both shown that focusing is possible in physiological conditions in the outer wells and provided preliminary evidence that focusing in the central wells of a multiwell potential is also possible beyond the assumptions used in Ref. [26].

ACKNOWLEDGMENT

This work was supported in part by the NSF under Grant No. PHY-1205788.

[1] L. Gammaitoni, P. Hänggi, P. Jung, and F. Marchesoni, Rev. Mod. Phys. **70**, 223 (1998).
[2] J. Kallunki, M. Dube, and T. Ala-Nissila, J. Phys.: Condens. Matter **11**, 9841 (1999).
[3] S. M. Bezrukov and I. Vodyanoy, Nature (London) **378**, 362 (1995).
[4] P. Hänggi, Chem. Phys. Chem. **3**, 285 (2002).
[5] R. K. Adair, Proc. Natl. Acad. Sci. USA **100**, 12099 (2003).
[6] I. Goychuk, P. Hänggi, J. L. Vega, and S. Miret-Artés, Phys. Rev. E **71**, 061906 (2005).
[7] I. Goychuk and P. Hänggi, Phys. Rev. Lett. **91**, 070601 (2003).
[8] K. Wiesenfeld and F. Jaramillo, Chaos **8**, 539 (1998).
[9] N. V. Agudov, A. V. Krichigin, D. Valenti, and B. Spagnolo, Phys. Rev. E **81**, 051123 (2010).
[10] M. Borromeo and F. Marchesoni, Phys. Rev. E **81**, 012102 (2010).
[11] A. Kolbus, A. Lemarchand, A. L. Kawczyński, and B. Nowakowski, Phys. Chem. Chem. Phys. **12**, 13224 (2010).
[12] F. Guo and Y. Zhou, Physica A **388**, 3371 (2009).
[13] F. Guo, X. F. Cheng, X. D. Yuan, and S. B. He, Adv. Mat. Res. **295–297**, 2143 (2011).
[14] J. H. Li and J. Luczka, Phys. Rev. E **82**, 041104 (2010).
[15] S. Miyamoto, K. Nishiguchi, Y. Ono, K. M. Itoh, and A. Fujiwara, Phys. Rev. B **82**, 033303 (2010).
[16] J. G. Orlandi and J. M. Sancho, Eur. Phys. J. E **29**, 329 (2009).
[17] M. J. Chacron and G. W. Slater, Phys. Rev. E **56**, 3446 (1997).
[18] C. R. Doering and J. C. Gadoua, Phys. Rev. Lett. **69**, 2318 (1992).
[19] O. Flomenbom and J. Klafter, Phys. Rev. E **69**, 051109 (2004).
[20] D. Li, W. Xu, X. Yue, and Y. Lei, Nonlinear Dyn. **70**, 2237 (2012).
[21] P. K. Ghosh, B. C. Bag, and D. S. Ray, J. Chem. Phys. **127**, 044510 (2007).
[22] A. Ichiki, Y. Tadokoro, and M. I. Dykman, Phys. Rev. E **85**, 031106 (2012).
[23] X. X. Wang and J. D. Bao, Phys. Rev. E **83**, 011127 (2011).
[24] G. J. Schmid, P. Reimann, and P. Hänggi, J. Chem. Phys. **111**, 3349 (1999).
[25] K. Lee and W. Sung, Phys. Rev. E **60**, 4681 (1999).
[26] M. M. Millonas and D. R. Chialvo, Phys. Rev. Lett. **76**, 550 (1996).
[27] A. Kargol and K. Kabza, Phys. Biol. **5**, 026003 (2008).
[28] B. Hille, *Ionic Channels of Excitable Membranes* (Sinauer, Sunderland, MA, 1992).
[29] F. Bezanilla, E. Perozo, and E. Stefani, Biophys. J. **66**, 1011 (1994).
[30] M. C. Mahato and A. M. Jayannavar, Physica A **248**, 138 (1998).
[31] P. K. Ghosh and D. S. Ray, J. Chem. Phys. **125**, 124102 (2006).
[32] E. Di Cera, J. Chem. Phys. **95**, 5082 (1991).
[33] M. C. Mahato and A. M. Jayannavar, Phys. Lett. A **209**, 21 (1995).
[34] P. E. Kloeden and E. Platen, *Numerical Solution of Stochastic Differential Equations* (Springer, Berlin, 1995).